

## Cell imaging using red fluorescent light-up probes based on an environment-sensitive fluorogen with intramolecular charge transfer characteristics†

Cite this: *Chem. Commun.*, 2014, 50, 9497Received 19th June 2014,  
Accepted 3rd July 2014

DOI: 10.1039/c4cc04654d

www.rsc.org/chemcomm

Guangxue Feng,‡<sup>ab</sup> Jie Liu,‡<sup>a</sup> Ruoyu Zhang<sup>a</sup> and Bin Liu\*<sup>ac</sup>

**We report a general strategy to design and synthesize red fluorescent light-up probes for cellular imaging based on a fluorogen with intramolecular charge transfer characteristics.**

Fluorescence imaging has become an indispensable tool in the study of living systems due to its high sensitivity, low cost, multiple parameters (*e.g.*, intensity, wavelength and lifetime) as well as activatable or multiplexed signals.<sup>1</sup> However, the photo-limiting interferences in biological media, such as autofluorescence, tissue absorption and scattering, limit fluorescence detection from being widely applied in practical settings. If the probes could be engineered to remain fluorescence silent and only be switched on in recognition of a specific biological event, it would provide a large signal-to-noise ratio with minimized background fluorescence.<sup>2</sup> On the other hand, employment of long wavelength fluorescent probes is also an alternative to reduce the photo-limiting interference due to the minimal interferential absorption and high tissue penetration ability.<sup>3</sup> As a result, it is of high importance to develop smart fluorescent probes possessing both long wavelength emission and the ability to significantly enhance their fluorescence in response to biological stimuli.

To date, several strategies have been employed to design fluorescent light-up probes for cellular imaging. One is to cage the fluorescent dye with photochemical labile groups, where the fluorescence is generated upon UV light irradiation.<sup>4</sup> The other example is dual labelled probes containing a fluorophore–quencher pair.<sup>5,6</sup>

When the fluorophore and the quencher are located within a specific distance, the fluorescence of the probe is quenched. Once they are separated by specific biological events, the fluorescence of the probe could be recovered. Another example is a singly labelled probe, which typically contains a fluorescence silent signal subunit that responds to an analyte or links to a binding unit/recognition site.<sup>7</sup> The molecular recognition process is often accompanied by fluorescence recovery. For example, some silent fluorophores can recognize target analytes, such as enzymes,<sup>8</sup> metal ions<sup>9</sup> or signalling molecules,<sup>10</sup> in biology to turn on the fluorescence. Probes containing fluorogens with aggregation-induced emission (AIE) characteristics also belong to this category. These probes are non-fluorescent when molecularly dissolved, but become highly fluorescent once aggregates are formed or upon restriction of intramolecular rotation induced by a biological event.<sup>11</sup> In addition, few probes containing environment sensitive fluorophores have also been developed,<sup>12</sup> which have weak fluorescence in polar media, and the fluorescence light-up occurs when the probe is bound to hydrophobic protein domains. So far, the AIE fluorogens and the environment sensitive dyes used for light-up probe design are limited to those with blue or green emission. It is highly desirable to develop specific fluorescent light-up probes with long wavelength emission for cell imaging.

One efficient way to design long wavelength emissive fluorophores is the combination of electron rich and electron deficient units to form a donor (D)–acceptor (A) structure.<sup>13</sup> The obtained molecules often possess intramolecular charge transfer (ICT) characteristics,<sup>14</sup> and their fluorescence is sensitive to the polarity of the environments, *e.g.*, lower fluorescence in high polar media.<sup>15</sup> One could expect that these molecules can be designed to have very low fluorescence in a highly polar environment (*e.g.*, aqueous environment), while the fluorescence is enhanced when the environment becomes hydrophobic or less polar. In addition, our previous studies have shown that conjugated polyelectrolytes with ICT characteristics have enhanced fluorescence upon aggregation due to their reduced exposure to polar environments.<sup>16</sup> These examples further inspire us to develop a new strategy to design and synthesize

<sup>a</sup> Department of Chemical and Biomolecular Engineering, National University of Singapore, Singapore 117576, Singapore. E-mail: cheliub@nus.edu.sg; Fax: +65-6779-1936

<sup>b</sup> Environmental Research Institute, National University of Singapore, 117411, Singapore

<sup>c</sup> Institute of Materials Research and Engineering, 3 Research Link, 117602, Singapore

† Electronic supplementary information (ESI) available: Experimental details, Lippert plot, titration and DFT calculation of DBT, NMR, EIMS, HPLC, LLS and photostability of DBT-KRRRQRRKKR, the CLSM image of EDBT treated cells. See DOI: 10.1039/c4cc04654d

‡ G. Feng and J. Liu contributed equally to this work.

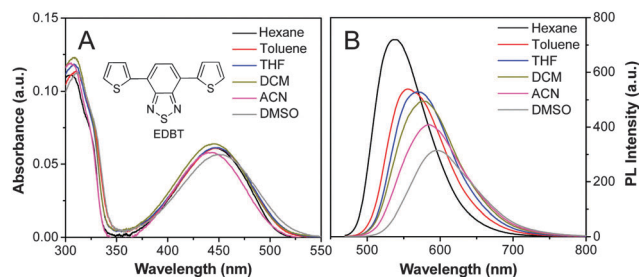
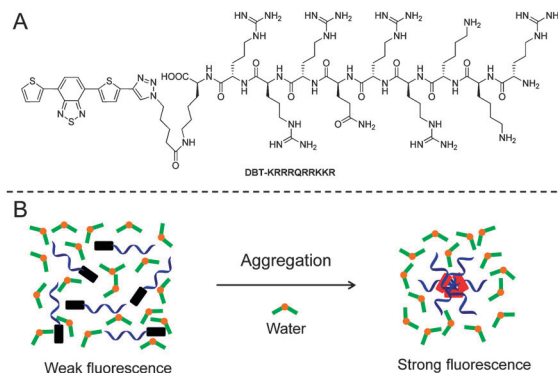


**Fig. 1** (A) UV-vis and (B) PL spectra of EDBT in hexane, toluene, tetrahydrofuran, dichloromethane, acetonitrile and dimethyl sulfoxide. [EDBT] = 2  $\mu$ M. The chemical structure of EDBT is shown in the inset of (A).

environment sensitive light-up probes by taking advantage of ICT characteristics. In this contribution, we selected thiophene as the electron donor and highly electron-deficient 2,1,3-benzothiadiazole as an electron acceptor to construct a donor-acceptor-donor (D-A-D) structured fluorophore. A water soluble peptide was further incorporated into one side of the fluorophore to impart the probe with good water solubility. After cell uptake, the fluorescence of the probe is significantly enhanced.

We first studied the ICT characteristics of 4-(5-ethynylthiophen-2-yl)-7-(thiophen-2-yl)-2,1,3-benzothiadiazole (EDBT, the chemical structure is shown in the inset of Fig. 1A), by measuring its absorption and emission spectra in solvents with different polarities (dielectric constant ( $\epsilon$ )). As shown in Fig. 1A, all the absorption spectra have maxima at  $\sim$ 453 nm, and there are no obvious changes observed in all six solvents. Along with an increase of  $\epsilon$ , the emission maxima, however, progressively red-shift from 542 nm in hexane ( $\epsilon$  = 2.0), to 563 nm in toluene ( $\epsilon$  = 2.4), 578 nm in tetrahydrofuran (THF,  $\epsilon$  = 7.5), 583 nm in dichloromethane (DCM,  $\epsilon$  = 9.1), 587 nm in acetonitrile (ACN,  $\epsilon$  = 36.6) and 597 nm in dimethyl sulfoxide (DMSO,  $\epsilon$  = 47.2), concomitant with a gradual decrease in the fluorescence intensity (Fig. 1B). The Lippert-Mataga plot<sup>15</sup> (Fig. S1 in the ESI<sup>†</sup>) shows that EDBT has small Stokes shifts in aprotic solvents (e.g. hexane) with low orientational polarizability, but with largely increased Stokes shifts over 5000  $\text{cm}^{-1}$  in polar solvents (e.g. DMSO). These results reveal that EDBT is an environment-polarity-sensitive fluorophore. Moreover, the fluorescence of EDBT can be effectively quenched in water to yield very low fluorescence (Fig. S2, ESI<sup>†</sup>), which provides us an opportunity to develop fluorescent light-up probes by taking advantage of the environment-polarity changes. The density functional theory (DFT) calculation of EDBT was also performed by using a suite of Gaussian 03 program. The lowest unoccupied molecular orbital (LUMO) of EDBT is dominated by the orbitals from the benzothiadiazole moiety, while the electron clouds of the highest occupied molecular orbital (HOMO) are mainly located on both thiophene and benzothiadiazole units (Fig. S3, ESI<sup>†</sup>). The difference in the electron cloud distribution shows intrinsic ICT properties, which is consistent with the fluorescence titration results.

We subsequently designed and synthesized the probe, DBT-KRRRQRRKKR, and the chemical structure is shown in Scheme 1A. A cell penetrating peptide KRRRQRRKKR was conjugated with EDBT to afford DBT-KRRRQRRKKR *via* a click



**Scheme 1** (A) Chemical structure of DBT-KRRRQRRKKR; (B) schematic illustration of the switching mechanism for the fluorescent light-up probe.

reaction. The detailed synthetic route and procedures are provided in Scheme S1 (ESI<sup>†</sup>). The chemical structures of key intermediates and the final probe were characterized by <sup>1</sup>H NMR, EIMS and HPLC (Fig. S4–S7, ESI<sup>†</sup>). The probe shows good solubility in aqueous media. The switching mechanism of the probe is proposed in Scheme 1B. When the probe is molecularly dissolved in aqueous media, its fluorescence is very weak due to strong ICT-induced fluorescence quenching. When the probe interacts with cell components or proteins after cell uptake, the increase in environment hydrophobicity will light-up the fluorescence.

The UV-vis absorption spectrum of DBT-KRRRQRRKKR was recorded in 150 mM phosphate buffered saline (PBS). As shown in Fig. 2A, DBT-KRRRQRRKKR has two absorption peaks centred at 325 and 462 nm, which arise as a result of a  $\pi$ - $\pi^*$  transition centred on the donor units along with the charge transfer between the donor (thiophene) and the acceptor (benzothiadiazole) units, respectively. The red-shifted absorption maximum of DBT-KRRRQRRKKR relative to EDBT reveals that the triazole ring formed after the click reaction also contributes to the effective conjugation length. As shown in Fig. 2B, the PL maxima of DBT-KRRRQRRKKR show clear red-shifts from 609 nm in ACN to 621 nm in DMSO and 650 nm in 150 mM PBS buffer ( $\epsilon$  = 80.1), accompanied with a decrease in the fluorescence intensity, indicating that the probe is indeed sensitive to the environment polarity.

To evaluate the capability of DBT-KRRRQRRKKR as a fluorescent light-up probe, the titration experiments were carried out in the cell medium upon addition of cell lysate. The PL spectra were obtained upon excitation at 462 nm. DBT-KRRRQRRKKR solution shows very weak fluorescence in the cell medium with an emission maximum at  $\sim$ 650 nm. Upon gradual addition of cell cytoplasmic lysate, the solutions exhibit enhanced bright red fluorescence, accompanied with a blue-shift of emission maxima from  $\sim$ 650 nm to 616 nm (Fig. 2C). The gradual blue-shift of emission maxima indicates that the microenvironment of the probe becomes relatively more hydrophobic, which is beneficial to suppress charge transfer-induced fluorescence quenching. The fluorescence change is also associated with aggregate formation, which is evidenced by the laser light scattering. The hydrodynamic size of aggregates

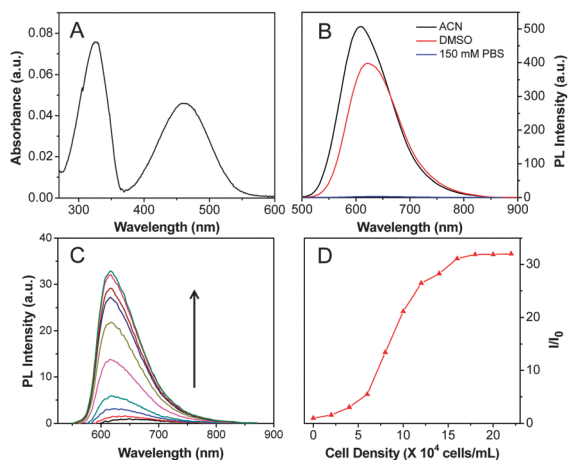


**Fig. 2** (A) UV-vis spectrum of DBT-KRRRQRRKKR in 150 mM PBS solution. (B) PL spectra of DBT-KRRRQRRKKR in ACN, DMSO, and 150 mM PBS solution. (C) PL spectra of DBT-KRRRQRRKKR in the presence of the cell lysate based on cell density ranging from 0 to  $2.2 \times 10^5$  cells per mL. (D) Titration experiments depicted by  $I/I_0$  as a function of cell lysate based on cell density.  $I$  is the maximum fluorescence intensity in the presence of cells, and  $I_0$  is the initial maximum fluorescence intensity of the probe alone. [DBT-KRRRQRRKKR] =  $2 \mu\text{M}$ .

formed between DBT-KRRRQRRKKR and the cell lysate increases from  $\sim 1$  nm to more than  $1 \mu\text{m}$  when the cell lysate based on the cell density is increased from 0 to  $2.2 \times 10^5$  cells per mL (Fig. S8, ESI<sup>†</sup>). It is worth noting that the maximum fluorescence intensity increases by  $\sim 32$ -fold relative to the probe alone in the absence of cell cytoplasmic lysate (Fig. 2D), indicating that the probe has a large signal-to-noise ratio, which is crucial for fluorescent light-up probes. The light-up probe exhibits almost no fluorescence change in the cell lysate when the pH is varied from 5 to 8 (Fig. S9, ESI<sup>†</sup>), revealing the insensitivity of DBT-KRRRQRRKKR to intracellular pH.

DBT-KRRRQRRKKR is subsequently used as a fluorescent light-up probe for live cell imaging. MCF-7 breast cancer cells were chosen as a model cell line for the fluorescence imaging study by confocal laser scanning microscopy (CLSM). After incubation with  $2 \mu\text{M}$  EDBT or DBT-KRRRQRRKKR at  $37^\circ\text{C}$  for 0, 1, 2, 3, and 4 h, respectively, the images were obtained upon excitation at 488 nm with red fluorescence signals collected above 560 nm. Almost no fluorescence is observed for MCF-7 cells upon incubation with EDBT alone (Fig. S10, ESI<sup>†</sup>), indicating that peptide conjugation is essential for cell uptake. On the other hand, when the images were immediately taken after the cells were incubated with  $2 \mu\text{M}$  DBT-KRRRQRRKKR (0 h), no fluorescence was observed (Fig. S11, ESI<sup>†</sup>), indicating that the probe exhibits very weak fluorescence in the culture medium outside the cell. As shown in Fig. 3, some fluorescence on the cell membrane is observed after 1 h incubation. As the incubation time gradually increases to 4 h, the bright red fluorescence is gradually spread through the whole cytoplasm even in the nucleus (Fig. 3). We also varied the DBT-KRRRQRRKKR concentrations for the cellular imaging. At lower concentration ( $0.5 \mu\text{M}$ ), the probe tends to stay longer on the cell membrane, while higher probe concentration ( $10 \mu\text{M}$ ) benefits fast cell uptake and quick

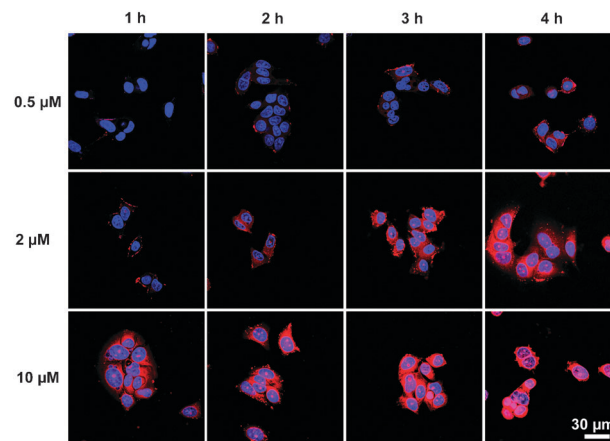


**Fig. 3** CLSM images of living MCF-7 cancer cells treated with DBT-KRRRQRRKKR at different concentrations for 1, 2, 3, and 4 h, respectively. The nuclei were pre-stained with nucleus staining dye Hoechst ( $5 \mu\text{g mL}^{-1}$ ) for 20 min. All the images share the same scale bar.

light up in the nucleus. The results coincide well with the literature on penetration peptide mediated cellular uptake, which occurs at two stages: binding to the membrane followed by disintegration of the membrane and internalization into the cytoplasm.<sup>17</sup> The fluorescence light-up in the nucleus is due to the nucleus localization signalling function of the peptide.

To study the mechanism of fluorescence light-up in cells, we also titrated DBT-KRRRQRRKKR with bovine serum albumin (BSA) or lipid (1,2-dipalmitoyl-*sn*-glycero-3-phosphocholine (DPPC)) (Fig. S12, ESI<sup>†</sup>). The probe showed similar fluorescence enhancement as that by titration with the cell lysate. Moreover, the probe showed instant fluorescence light-up upon mixing with the cell lysate, and the fluorescence remained almost unchanged for 4 h. As the peptide hydrolysis takes time, the results indicate that the light-up mechanism should be mainly due to the interaction between the probe and cellular proteins or the membrane, which provides a hydrophobic microenvironment for probe fluorescence enhancement. These results suggest that DBT-KRRRQRRKKR can serve as a potential cell uptake-mediated fluorescent light-up probe for cell imaging.

Photostability comparisons among DBT-KRRRQRRKKR, Alexa fluor 488 and fluorescein were evaluated under continuous laser scanning upon illumination at 488 nm with a power of 1.25 mW. Only  $\sim 12\%$  fluorescence intensity loss was observed for DBT-KRRRQRRKKR after 10 min illumination, which is better than Alexa fluor 488 ( $\sim 23\%$  signal loss) and fluorescein ( $\sim 100\%$  signal loss) (Fig. S13, ESI<sup>†</sup>), suggesting that DBT-KRRRQRRKKR has good photostability. In addition, the cytotoxicity results evaluated by MTT assays reveal that the cell viabilities still remain above 80% after 48 h of incubation with a  $5 \mu\text{M}$  probe (Fig. S14, ESI<sup>†</sup>).

In conclusion, we used a new strategy to design and synthesize a cell uptake-mediated red fluorescent light-up probe for cell imaging. The fluorophore has a D-A-D structure, which allows us to take advantage of the ICT characteristics to light up its fluorescence by changing the environment polarity from polar to non-polar (*e.g.* upon cellular uptake and aggregate

formation). This work provides a general design principle to develop red fluorescent light-up probes for cellular imaging without washing steps. In the future, we will use such design principles to develop NIR fluorescent light-up probes with targeting ability through conjugation with specific ligands for targeted cellular imaging.

The authors are grateful to the Singapore National Research Foundation (R279-000-390-281), Singapore Ministry of Defence (R279-000-340-232), Institute of Materials Research and Engineering of Singapore (IMRE/8P1103), and the Economic Development Board (Singapore-Peking-Oxford Research Enterprise, COY-15-EWI-RCFSA/N197-1) for financial support.

## Notes and references

- (a) R. Weissleder and M. J. Pittet, *Nature*, 2008, **452**, 580; (b) K. Park, S. Lee, E. Kang, K. Kim, K. Choi and I. C. Kwon, *Adv. Funct. Mater.*, 2009, **19**, 1553.
- Q. T. Nguyen, E. Olson, T. A. Aguilera, T. Jiamg, M. Scadeng, L. G. Ellies and R. Y. Tsien, *Proc. Natl. Acad. Sci. U. S. A.*, 2010, **107**, 4317.
- (a) J. V. Frangioni, *Curr. Opin. Chem. Biol.*, 2003, **7**, 626; (b) S. A. Hilderbrand and R. Weissleder, *Curr. Opin. Chem. Biol.*, 2010, **14**, 71; (c) M. A. Pysz, S. S. Gambhir and J. K. Willmann, *Clin. Radiol.*, 2010, **65**, 500.
- (a) T. J. Mitchison, *J. Cell Biol.*, 1989, **109**, 637; (b) T. J. Mitchison, K. E. Sawin, J. A. Theriot, K. Gee and A. Mallavarapu, *Methods Enzymol.*, 1998, **291**, 64; (c) V. N. Belov, C. A. Wurm, V. P. Boyarskiy, S. Jakobs and S. W. Hell, *Angew. Chem., Int. Ed.*, 2010, **49**, 3520.
- M. Verdoes, K. O. Bender, E. Segal, W. A. van der Linden, S. Syed, N. P. Withana, L. E. Sanman and M. Bogoy, *J. Am. Chem. Soc.*, 2013, **135**, 14726.
- J. R. Lakowicz, *Principles of Fluorescence Spectroscopy*, Springer, New York, 3rd edn, 2006.
- M. E. Jun, B. Roy and K. H. Ahn, *Chem. Commun.*, 2011, **47**, 7583.
- M. Kamiya, H. Kobayashi, Y. Hama, Y. Koyama, M. Bernardo, T. Nagano, P. L. Choyke and Y. Urano, *J. Am. Chem. Soc.*, 2007, **129**, 3918.
- (a) V. Dujols, F. Ford and A. W. Czarnik, *J. Am. Chem. Soc.*, 1997, **119**, 7386; (b) T. Cheng, Y. Xu, S. Zhang, W. Zhu, X. Qian and L. Duan, *J. Am. Chem. Soc.*, 2008, **130**, 16160.
- Y. Qian, J. Karpus, O. Kabil, S. Y. Zhang, H. L. Zhu, R. Banerjee, J. Zhao and C. He, *Nat. Commun.*, 2011, **2**, 495.
- (a) D. Ding, K. Li, B. Liu and B. Z. Tang, *Acc. Chem. Res.*, 2013, **46**, 2441; (b) H. Shi, J. Liu, J. Geng, B. Z. Tang and B. Liu, *J. Am. Chem. Soc.*, 2012, **134**, 9569; (c) H. Shi, R. T. K. Kwok, J. Liu, B. Xing, B. Z. Tang and B. Liu, *J. Am. Chem. Soc.*, 2012, **134**, 17972; (d) Y. Hong, J. W. Y. Lam and B. Z. Tang, *Chem. Commun.*, 2009, 4332.
- (a) A. Toutchkine, V. Kraynov and K. Hahn, *J. Am. Chem. Soc.*, 2003, **125**, 4132; (b) P. Nalbant, L. Hodgson, V. Kraynov, A. Toutchkine and K. M. Hahn, *Science*, 2004, **305**, 1615; (c) C. T. MacNevin, D. Gremyachinskiy, C. W. Hsu, L. Li, M. Rougie, T. T. Davis and K. M. Hahn, *Bioconjugate Chem.*, 2013, **24**, 215.
- K. R. J. Thomas, J. T. Lin, M. Velusamy, Y.-T. Tao and C.-H. Chuen, *Adv. Funct. Mater.*, 2004, **14**, 83.
- G. L. Gibson, T. M. McCormick and D. S. Seferos, *J. Am. Chem. Soc.*, 2012, **134**, 539.
- (a) G. Weber and F. J. Farris, *Biochemistry*, 1979, **18**, 3075; (b) G. L. Gibson, T. M. McCormick and D. S. Seferos, *J. Am. Chem. Soc.*, 2012, **134**, 539.
- K. Y. Pu, L. Cai and B. Liu, *Macromolecules*, 2009, **42**, 5933.
- S. Piantavigna, G. A. McCubbin, S. Boehnke, B. Graham, L. Spiccia and L. L. Martin, *Biochim. Biophys. Acta, Biomembr.*, 2011, **1811**, 1807.